MHD Simulations with Resistive Wall and Magnetic Separatrix

H.R. Strauss

New York University, New York, New York

A. Pletzer, W. Park, S. Jardin, J. Breslau, G. Y. Fu

Princeton University Plasma Physics Laboratory, Princeton, New Jersey

L. Sugiyama

MIT, Cambridge, MA

Abstract

A number of problems in resistive MHD magnetic fusion simulations describe plasmas with three regions: the core, the halo region, and the resistive boundary. Treating these problems requires maintainance of an adequate resistivity contrast between the core and halo. This can be helped by the presence of a magnetic separatrix, which in any case is required for reasons of realistic modeling. An appropriate mesh generation capability is also needed to include the halo region when a separatrix is present. Finally a resistive wall boundary condition is required, to allow both two dimensional and three dimensional magnetic perturbations to penetrate the wall. Preliminary work is presented on halo current simulations in ITER. The first step is the study of VDE (vertical displacement event) instabilities. The growth rate is consistent with scaling inversely proportional to the resistive wall penetration time. The simulations have resistivity proportional to the $-3/2$ power of the temperature. Simulations have been done with resistivity contrast between the plasma core and wall of 1000 times, to model the vacuum region between the core and resistive shell. Some 3D simulations are shown of disruptions competing with VDEs. Toroidal peaking factors are up to about 3.

Key words: MHD; Resistive Wall; Magnetic separatrix

[1] This work was supported by USDOE.

1 Introduction

In several resistive MHD simulational problems, the plasma model consists of three regions: the plasma core, the plasma halo region, and a resistive wall connecting the plasma to an extenal vacuum magnetic field.

Example problems having these regions are VDEs and halo current simulations in ITER, with the aim of determining maximum wall stresses caused by asymmetric forces during disruptions. Other problems with some of these features is the effect of error magnetic fields on toroidal rotation, and the evolution of resistive wall modes. Another related category of problem is the development of external kink modes, particularly in compact quasi axisymmetric stellarators.

Tackling these problems requires a resistive MHD code to have three numerical capabilities. First, a three dimensional time dependent resistivity is needed, with adequate contrast of maximum and minimum values. Second, mesh generation is required within a realistic boundary, which may contain a divertor. Third, a resistive wall boundary condition is needed, with a method of solving the external vacuum magnetic field.

These capabilities have been developed for the M3D code [1,2]. The resistivity is proportional to the $-3/2$ power of the temperature. Simulations have been done with temperature contrast between the plasma core and wall of 100, to model the halo region between the core and resistive shell.

The M3D code includes resistive wall boundary conditions, which match the solution inside the resistive wall to the exterior vacuum solution. The exterior problem is solved with a Green's function method, using A. Pletzer's GRIN code [3].

As a computational example of a problem requiring these capabilities, preliminary work is presented on halo current simulations in ITER[4]. The first step is the study of VDE (vertical displacement event) instabilities[5]. The growth rate is consistent with scaling inversely proportional to the resistive wall penetration time. Some 3D simulations are shown of disruptions competing with VDEs. The toroidal peaking factor[6] can be as high as 3.

2 Resistivity Model

A main problem is to have a time dependent resistivity, which is nearly constant along magnetic field lines. In two dimensions, and in mildly three dimensional cases,

a magnetic separatrix can provide an adequate temperature contrast. Open field lines are in contact with the wall, which is held at a relatively low constant temperature. Inside the separatrix, if the cross field thermal conduction is small, the temperature can be maintained at much higher values.

In M3D, the temperature is evolved with the "artificial sound" [7] model, which resembles Landau fluid models [8]

$$\frac{\partial T}{\partial t} = -\mathbf{v} \cdot \nabla T - \gamma_0 T \nabla \cdot \mathbf{v} + \mathbf{B} \cdot \nabla q_{\|}$$

$$\frac{\partial q_{\|}}{\partial t} = -\frac{1}{\tau_a} - \mathbf{B} \cdot \nabla T q_{\|}$$

where $\gamma_0 = 2/3$, T is the temperature, $\mathbf{v}$ is the velocity, $\mathbf{B}$ is the magnetic field, $q_{\|}$ is the heat flux, and τ_a is a constant. In Landau fluid models, τ_a is a more complicated quantity, but it is difficult to generalize to realistic three dimensional magnetic fields.

In three dimensional disruption calculations, the magnetic field becomes stochastic and no longer can isolate the halo region from the core. The regions mix and the core is cooled, resulting in a thermal quench. In turn this causes a current quench, because of the high resistivity.

3 Mesh Generation

M3D combines a two dimensional unstructured mesh with finite element discretization in poloidal planes [9], with a pseudo spectral representation in the toroidal direction. An unstructured mesh similar to that used in the calculations is shown in Fig.2(a). The boundary geometry is realistic, for example the ITER - FEAT first wall[10]. The halo part of the mesh containing the open magnetic field lines was made using the ellipt2d package [11], which incorporates the Triangle [12] mesh generation code. The core part of the mesh is aligned with the equilibrium magnetic flux surfaces. It is possible to generate the mesh and initialize using EQDSK equilibrium files. These files contain data describing the curves of the outer wall and the last closed flux surface. These curves are filled in with an unstructured, but good quality mesh by Triangle, which carries out a Delauney triangulation of this region. Extra points are added to the boundaries to improvem mesh quality and ensure the desired resolution. The region inside the last closed flux surface is triangulated by M3D. The EQDSK file contains the poloidal flux function ψ on a cartesian grid, and the corrdinates of the magnetic axis. M3D uses this information to produce a mesh with sides aligned with contours of constant ψ, as well as rays connecting the magnetic axis to the mesh points on the last closed flux surface.

4 Resistive Wall Boundary Conditions

The plasma is bounded by a thin resistive wall. Surrounding this is an outer vacuum region, which can contain external current sources.

The vacuum field is represented as

$$\mathbf{B}_v = \nabla\psi_v \times \nabla\phi + \nabla\lambda + I_0\nabla\phi \tag{1}$$

where I_0 is a constant which is equal to the constant part of I in the plasma. The reason for I_0, as well as ψ_v, is to be able to match the vacuum solution to a plasma equilibrium with a net current, and net toroidal magnetic field. The function ψ_v depends on the poloidal coordinates R, Z and is independent of toroidal angle ψ. It satisfies the vacuum Grad Shafranov equation $\Delta^*\psi_v = 0$.

To satisfy $\nabla \cdot \mathbf{B}_v = 0$, $\nabla^2\lambda = 0$. On the resistive wall boundary, integrating $\nabla \cdot \mathbf{B}$ across the thin shell gives the requirement that the normal component of magnetic field is continuous at the wall. This gives a boundary condition to determine the vacuum field.

The vacuum field is solved by the GRIN code. From Green's identity one has an integral equation relating $\partial\psi_v/\partial n$ to given ψ_v, and λ_n to given $\partial\lambda_n/\partial n$ on the boundary contour [13] When discretized, these integral equations become matrix equations which are set up and solved by GRIN. Given a set of boundary points, R_i, Z_i

$$(\frac{\partial\psi_v}{\partial n})_i = \sum_j K^0_{ij}\psi_{pj} + S_i, \tag{2}$$

$$\lambda^n_i = \sum_j K^n_{ij}(\mathbf{B}^p \cdot \hat{n})_j \tag{3}$$

where K^0_{ij}, K^n_{ij} are matrices that can be precomputed given the set of boundary points. The source term S in (3) can be obtained from the applied external currents, or else using the "virtual casing" method. In this method we first perform an ideal equilibrium calculation, with $\psi = 0$ on the boundary. Equating $\partial\psi_v/\partial n = \partial\psi_p/\partial n$, the source term required for equilibrium is found from $S = \partial\psi_p/\partial n$ where the right side is obtained from the ideal equilibrium.

Now the magnetic field components in the plasma have to be matched using resistive evolution at the inner boundary, which is a thin resistive shell of thickness δ and

resistivity η_w. Ohm's Law at the resistive wall is

$$\frac{\partial \mathbf{A}}{\partial t} = \nabla\Phi + \frac{\eta_w}{\delta}\hat{n} \times [[\mathbf{B}]].$$

In addition, a toroidal electric field is applied to balance resistive diffusion. An example of the temperature in an equilibrium, with "virtual casing" source terms in the boundary conditions, is shown in Fig.1(a).

5 VDE and Disruption Simulations

The VDE instability growth rate is proportional to the wall resistivity η_w. This scaling is consistent with simulations, as will be shown below. To get the scaling it seems necessary to be in a regime in which the core resistive decay time τ_{core} is longer than the wall penetration time τ_w, which in turn is longer than the halo resistive decay time τ_{halo}, $\tau_{core} > \tau_w > \tau_{halo}$. Here $\tau_{core} = S\tau_A$, and $\tau_{halo} = (T_{halo}/T_{core})^{3/2}\tau_{core}$, where $\tau_A = R/v_A$ is the Alfvén time, R is the major radius, v_A is the Alfvén velocity, T_{halo}, T_{core} are temperatures in the halo and core respectively, $S = a^2 v_A/(\eta R) = 10^4$ in the simulations, where a is the geometric half width in the midplane, and S is the initial value at the magnetic axis. For over two orders of magnitude variation in η_w/δ_w, the growth rate of the VDE scales as $\gamma = 4.0\eta_w/\delta_w$. The growth rate γ as a function of η_w/δ_w is shown in Fig.2(b).

The temperature in the nonlinear stage of the VDE is shown in Fig.1(b) at time $t = 103\tau_A$, as the plasma is pulled into the divertor.

The halo current is the poloidal current flowing into the resistive wall. The normal component of the poloidal current integrated over the wall, I_h, is $I_h(\phi) = \frac{1}{2}\int |\hat{n}\cdot\mathbf{J}|Rdl$ Half the absolute value is taken in the integrand because $\nabla\cdot\mathbf{J} = 0$ implies the total normal current is zero when integrated over the wall and the toroidal angle ϕ. The toroidal peaking factor [6] is defined as the maximum of $I_h(\phi)$ divided by its toroidal average $< I_h >= 1/(2\pi)\int I_h d\phi$, that is, $tpf = I_{h(max)}/ < I_h >$. In the following simulation, $tpf \approx 2$.

It is useful to normalize halo current to total plasma current. The halo current fraction F_h will be defined as the ratio $F_h =< I_h > / < I_\phi >$, where the denominator is $I_\phi = \int J_\phi dRdZ$.

In three dimensional simulations, disruptions can occur. In one scenario, a disruption causes a thermal quench, which in turn causes a current quench. This is accompanied by a VDE.

The following calculation is an example of this scenario. The initial state has $q = 0.6$ on axis, with a $q = 1$ inversion radius including most of the core plasma. This is internal kink unstable. When the instability is sufficiently nonlinear, toroidal coupling to other modes causes a disruption. The plasma cools because of transport along stochastic field lines. This raises the resistivity and dissipates the current. This is acompanied by a VDE. The time history of the the normalized peak current and peak temperature in Fig.3(a). The temperature quench proceeds the current quench. The current, plotted with a dashed line, declines in value more slowly than the temperature, shown as a solid line. The time history of the toroidal peaking factor is shown in Fig.3(b), The toroidal peaking factor almost reaches 3, but most of the time oscillates around 2. The dashed curve in Fig.3(b) is the halo current fraction F_h multiplied by 10 to be easily read. The halo current peaks at 0.4 but then decays to about 0.1. It should be remarked that this is the instantaneous halo current fraction; both halo current and toroidal current are evolving in time. The temperature is shown at the time $t = 113\tau_A$ in Fig.1(c). After the disruption and expansion to the wall, the plasma rapidly cools. This tends to quench halo current. The halo current in this case is small.

6 Summary and Conclusion

A number of problems in resistive MHD magnetic fusion simulations describe plasmas with three regions: the core, the halo region, and the resistive boundary. Treating these problems requires maintainance of an adequate resistivity contrast between the core and halo. This can be helped by the presence of a magnetic separatrix, which in any case is required for reasons of realistic modeling. An appropriate mesh generation capability is also needed to include the halo region when a separatrix is present. Finally a resistive wall boundary condition is required, to allow both two dimensional and three dimensional magnetic perturbations to penetrate the wall.

M3D simulations have been done of VDEs and halo currents produced by disruptions. A resistive wall boundary condition was applied on a boundary having the shape of the ITER - FEAT first wall. The spatially and temporally varying resistivity was computed proportional to the $-3/2$ power of temperature. A temperature contrast of 100 between the plasma core and the edge was applied.

Two dimensional simulations of VDEs confirmed that the growth rate is proportional to the wall resistivity, over two orders of magnitude where the linear scaling assumptions are valid.

In three dimensional simulations, disruptions were initiated by a large inversion radius internal kink. Thermal transport along a stochastic magnetic field caused a thermal

quench, followed by a current quench and a VDE. The toroidal peaking factor could be as high as 3, and oscillated around 2.

References

[1] PARK, W., BELOVA, E.V., FU, G.Y., TANG, X.Z., STRAUSS, H.R., SUGIYAMA, L.E., "Plasma Simulation Studies using Multilevel Physics Models" Phys. Plasmas **6** 1796 (1999).

[2] SUGIYAMA, L.E., PARK, W., STRAUSS, H.R., HUDSON, S.R, STUTMAN, D., TANG, X.Z., Studies of Spherical Tori, Stellarators and Anisotropic Pressure with M3D, Nucl. Fusion (2001).

[3] http://w3.pppl.gov/rib/repositories/NTCC/catalog/Asset/grin.html

[4] Perkins, F. W., Post, D. E., Uckan, N. A., Azumi, M., Campbell, D. J., Ivanov, N., Sauthoff, N. R., Wakatani, M., Nevins, W.M., Shimada, M., and Van Dam, J., editors, "ITER Physics Basis," Nuclear Fusion 39, 2137 (1999).

[5] Sayer, R.O., Peng, Y-K. M., Jardin, S. C., Kellman, A. G., Wesley, J. C., "TSC plasma halo simulation of a DIII-D vertical displacement event," Nuclear Fusion 33, 969 (1993).

[6] Pomphrey, N., Bialek, J., Park, W., "Modeling the toroidal asymmetry of poloidal halo currents," Nuclear Fusion 38, 449 (1998).

[7] PARK, W., MONTICELLO, D., STRAUSS, H., MANICKAM,

[8] P. B. Snyder, G. W. Hammett, and W. Dorland, Phys. Plasmas 4, 3974 (1997). Phys. Fluids **29** (1986) 1171.

[9] STRAUSS, H.R. and LONGCOPE, W., An Adaptive Finite Element Method for Magnetohydrodynamics, J. Comput. Phys. 147, 318 - 336 (1998).

[10] Gribov, Y., private communication.

[11] Pletzer, A., "Python & Finite Elements", Dr. Dobb's Journal #334, p. 36 (March 2002) http://ellipt2d.sourceforge.net

[12] J. R. Shewchuk, Computational Geometry: Theory and Applications 22, 21 - 74 (2002)

[13] Chance, M., Phys. Plasmas **4**, 2161 (1997).

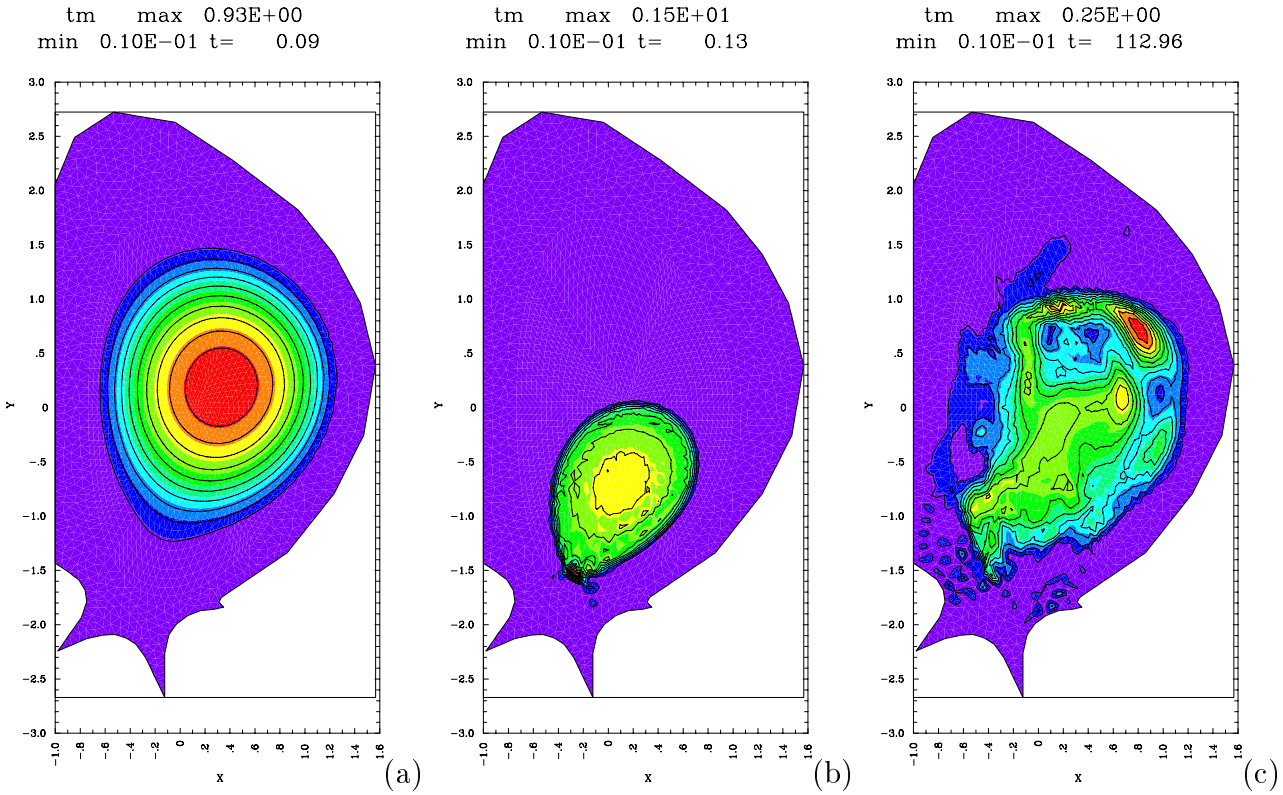

Fig. 1. (a) temperature at t = $0t_A$ (b) temperature at t = $103t_A$ in a 2D VDE (c) temperature at t = $113t_A$ in a 3D disruption

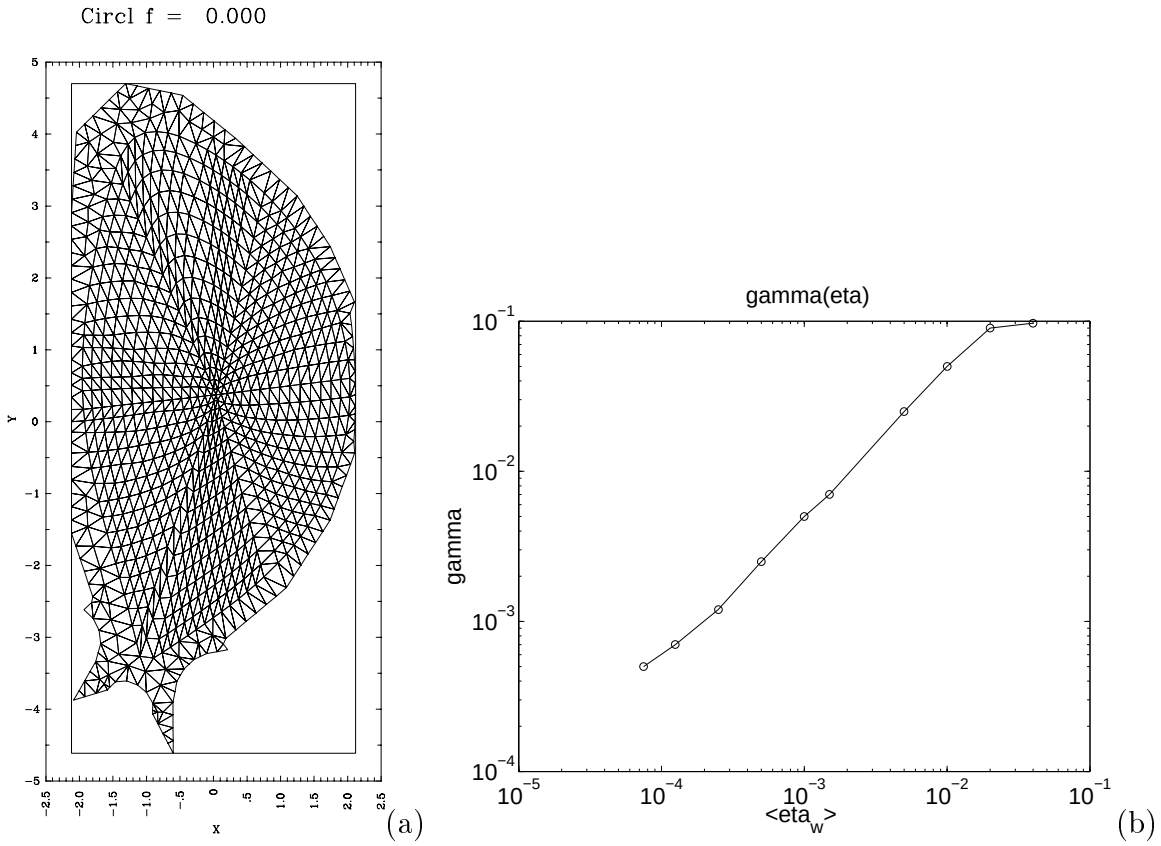

Fig. 2. (a) Mesh (b) Growth rate of VDEs vs. η_w/δ_w

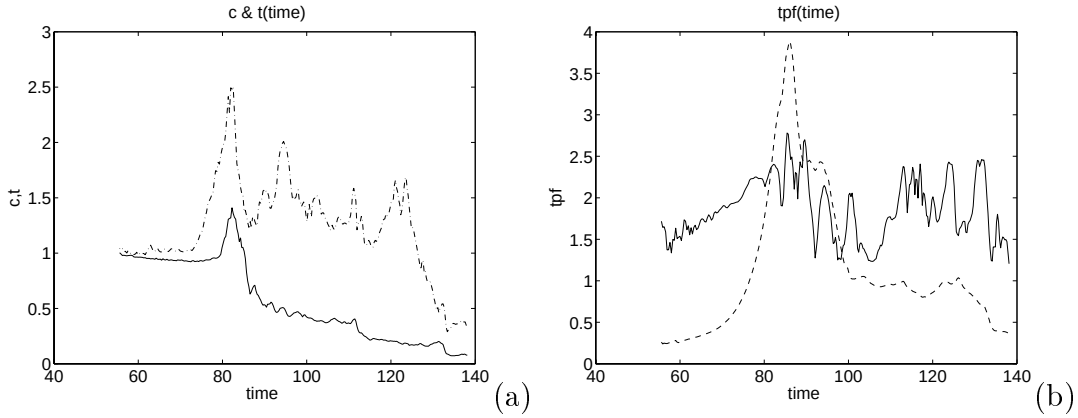

Fig. 3. (a) normalized peak toroidal current (dotted line) and peak temperature vs. time (b) toroidal peaking factor tpf (solid line) and halo current fraction times ten, $10F_h$, (dashed line) vs. time